Co-published by
Institute of Fluid-Flow Machinery
Polish Academy of Sciences
Committee on Thermodynamics and Combustion
Polish Academy of Sciences

http://www.imp.gda.pl/archives-of-thermodynamics/

Investigating the effect of an inclined magnetic field on heat and mass transmission in turbulent squeeze flow of UCM fluid between parallel plates

Sreenivasa Somireddy Reddy[a], Kamatam Govardhan[b], Ganji Narender[c*], Santoshi Misra[d]

[a]Department of Humanities and Science (Mathematics), Viganana Bharathi Institute of Technology, Hyderabad-501301, Telangana, India
[b]Department of Mathematics, GITAM University, Hyderabad-502329, Telangana, India
[c]Department of Humanities and Sciences (Mathematics), CVR College of Engineering, Hyderabad-501510, Telangana, India
[d]Department of Mathematics, St. Ann's College for Women, Hyderabad, Telangana, India
*Corresponding author email: gnriimc@gmail.com

Received: 23.11.2023; revised: 21.06.2024; accepted: 10.09.2024

Abstract

This paper investigates the effects of an inclined magnetic field on heat and mass transfer in turbulent squeeze flow of a viscoelastic fluid with an upper-convected Maxwell model. Squeezing flow is an important phenomenon in various industrial and mechanical processes related to flows between parallel surfaces. Mathematical modelling for the law of conservation of mass, momentum, heat and concentration of nanoparticles is executed. The study employs a system of partial differential equations to describe the flow issue. Governing nonlinear partial equations are reduced into nonlinear ordinary differential equations. The modelled equations are then solved numerically by utilizing the efficient Adams-Moulton method of the fourth order based on the shooting technique using the Fortran programming language. Numerical results are compared with another numerical approach and an excellent agreement is observed. The effects of various factors on the non-dimensional velocity, temperature, and concentration patterns are presented using graphs, while tables are used to assess the numerical values of the skin friction, Nusselt and Sherwood numbers. It is found that the temperature profile decreases as the compression parameter increases but increases with an increase in the Eckert number. The results of this study could be useful in designing heat and mass transfer equipment for applications in viscoelastic fluid flows under an inclined magnetic field.

Keywords: Magnetic field; Upper-convected Maxwell (UCM) fluid; Chemical reaction parameter; Viscous dissipation; Squeezing parameter; Adams-Moulton method

Vol. 45(2024), No. 4, 169–178; doi: 10.24425/ather.2024.152006

Cite this manuscript as: Reddy, S.S., Govardhan, K., & Narender, G. (2024). Investigating the effect of an inclined magnetic field on heat and mass transmission in turbulent squeeze flow of UCM fluid between parallel plates. *Archives of Thermodynamics*, 45(4), 169–178.

1. Introduction

The study of mass and heat transmission with various physical factors has attracted more attention in recent years as it occurs in a wide range of industries, including food processing, lubricant systems, hydrodynamic machinery, chemical processing equipment, and polymer processing. The impact of extrusion and squeezing factors on the rate of heat conduction of the compressed viscous fluid between two parallel plates was reported by Duwairi et al. [1]. They found that increasing the squeezing parameter caused the local coefficient of friction to reduce and the rate of heat conduction to increase, whereas increasing the extrusion parameter caused the rate of heat transfer to decline and the skin friction coefficient to increase.

In the study conducted by Kai-Long Hsiao [2], the focus was on the incompressible mixed convection 2D flow of a Maxwell fluid over an extending surface. The author specifically investigated the physical properties of energy conversion, conjugate mass transfer and heat transfer, considering radiative thermal effects. Ahmadi et al. [3] studied the unsteady flow of nanofluids and the transfer of heat by a uniformly moving disc. Given that the unstable parameter is a key component of the velocity pro-

Nomenclature

B_m – magnetic flux density, A/m
C – concentration, mol/m^3
C_f – skin friction coefficient
D – diffusion coefficient, m^2/s
Ec – Eckert number
f, f' – dimensionless velocity components
k – thermal conductivity, W/(m K)
K_1 – rate of reaction, 1/s
Nu – Nusselt number
p – pressure, Pa
Pr – Prandtl number
S – squeezing number
Sc – Schmidt number
Sh – Sherwood number
T – temperature of the fluid, K
T_H – temperature of the upper wall, K
u – velocity in x direction, m/s
v – velocity in y direction, m/s
x, y – Cartesian coordinates, m

Greek symbols

α – thermal diffusivity, m^2/s
γ – chemical reaction parameter
η – dimensionless coordinate
θ – dimensionless temperature
λ_r – viscoelastic parameter
ν – kinematic viscosity, m^2/s
μ – dynamic viscosity, Pa s
ρ – fluid density, kg/m^3
σ – electrical conductivity, S/m
ϕ – dimensionless concentration
ω – inclination angle, rad

Abbreviations and Acronyms

ADM– Adomian decomposition method
BCs – boundary conditions
HAM– homotopy analysis method
IVP – initial value problem
MHD– magnetohydrodynamics
ODEs– ordinary differential equations
PDEs– partial differential equations
UCM– upper-convected Maxwell

file, it has been suggested that raising this parameter will improve the velocity profile. In addition to the magnetic effect and chemical reaction, Afify [4] addressed the mass transfer in a convective, incompressible and electrically conducting movement of viscous fluid in the direction of expanding surfaces. According to this research, as the magnetic component is increased, the friction coefficient rises while the Nusselt and Sherwood numbers fall.

A substance droplet's mobility can be explained by the squeeze-flow process. Squeezing flow has many uses in industry and sciences, including rheological testing, connecting composite materials, hot plate welding, etc. In the presence of slip impact, Bhatta et al. [5] noticed the unsteady compression of water-based nanofluid flow between two plates held parallel to one another. It was found that a rise in the Lewis number caused a fall in the proportion of nanoparticles. Adesanyao et al. [6] conducted a study on the unsteady MHD compressing Eyring-Powell fluid flow over an infinite channel. Their findings indicated that with an increase in the chemical reaction parameter, the concentration profile decreases. The researchers came to the additional conclusion that while the rate of heat transmission declines with heat absorption and compressed channel walls, it increases with the expansion of thermal radiation, channel walls, and internal heat production parameters. Farooq et al. [7] described the effect of melting heat transfer in the compressing flow of nanofluid over a Darcy porous medium. They discovered that for the prevalent thermophoresis parameter values, the temperature distribution rises.

Hayat et al. [8] conducted a study on the flow of an incompressible micropolar fluid confined between two parallel plates, considering the magnetic effect. Mahmood et al. [9], on the other hand, investigated the heat transfer and flow characteristics over a sensor surface submerged in a squeezed channel. Their findings revealed that increasing suction through the sensor surface leads to an increase in heat transfer and skin friction coefficient. Conversely, an increase in injection has the opposite effect, decreasing the skin friction and heat transfer coefficient. Mohyud-Din et al. [10] examined the MHD flow of a squeezing fluid between two plates held parallel to one another, one of which is impervious and the other porous. Ojjela et al. [11] provided an explanation of the entropy production caused by the influence of a magnetic field on an unsteady incompressible 2D squeezing flow and the mass transfer of Casson fluid between two plates kept parallel to one another. They used the Prandtl and Hartmann numbers to evaluate whether the fluid's temperature was raised, and its content was reduced.

Sheikholeslami et al. [12] utilized the Adomian decomposition technique (ADM) to determine the analytical solution for the unsteady flow of nanofluid compressed between two parallel sheets. It was determined that the Nusselt number and nanoparticle volume fraction have a straight relationship; otherwise, when the two plates travel together, they have an opposite relationship with the squeezing number. Saltwater, liquid metals, electrolytes and plasmas are a few examples of electrically conducting fluids that are studied in magnetohydrodynamics for their magnetic characteristics and activity. According to Gholinia et al. [13], who examined the effects of various physical factors on Eyring-Powell fluid, including slip flow, magnetic fields, and homogeneous and heterogeneous processes brought on by spinning discs, the temperature profile decreases as the pressure increases. A 2D second-degree fluid flow between two parallel plates that was unsteady was noticed by Hayat et al. [14] to be affected by magnetism.

Jha and Aina [15] computed an approximate solution for an incompressible, viscous, electrically conducting fluid in a vertical microporous channel created by electrically non-conducting vertical slabs held parallel to one another in the presence of induced magnetic effects. They observed that the suction or injection measure increases fluid velocity and slip velocity. Additionally, it was found that as the magnetic component and Hartmann

number rise, the volume flow rate decreases.

In addition to the magnetic effect, Khan et al. [16] looked at the heat transmission in the nanofluid flow between two plates that were kept parallel to one another. They observed that the form component has no impact on the fluid velocity. Additionally, it was found that nanoparticles with a greater shape factor would raise temperatures and slow down heat transmission. With the aid of volume portions of nanoparticles, radiation, chemical processes and viscous dispersion, Mabood et al. [17] provided the computational solution of stagnation point flow of MHD nanofluid based on water (Cu and Al_2O_3) over a porous surface. The homotopy perturbation technique was used by Siddiqui et al. [18] to calculate the solution for an unsteady 2D squeezing fluid flow of MHD between two parallel plates. They observed that for both a constant value and for various values of the magnetic parameter, the velocity curve increases monotonically.

According to slip conditions at the boundaries, Abbasi et al. [19] showed the MHD flow of UCM fluid over a porous material. They discovered a correlation between a decline in the velocity curve and a rise in the Hartmann number. A two-dimensional, incompressible, constant flow through a porous surface conduit was studied by Choi et al. [20] to determine how inertia and viscoelasticity interacted. The 2D boundary layer of UCM fluid over a porous conduit with chemical processes was studied by Hayat and Abbas [21]. They came to the conclusion that the motion behaves differently for rising Reynolds number values in viscoelastic fluid. The similarity solutions for the unstable boundary layer flow and heat transfer in a Maxwell fluid flowing over a permeable stretching sheet in the presence of a heat source or sink were examined by Mukhopadhyay and Vajravelu [22]. For the rising levels of the Maxwell fluid and magnetic field, they observed a decrease in the velocity field.

Prasad et al. [23] conducted a study on the effects of thermal conductivity, internal heat source and heat sink on the MHD flow and heat transfer in the stretching surface of UCM fluid. The findings revealed that, when temperature-dependent thermo-physical properties were considered, increasing the magnetic parameter and Maxwell parameter led to a reduction in the velocity profile within the boundary layer. Additionally, they observed that thermal conduction and the presence of a heat source/sink raised the temperature in the flow region. In another study, Sadeghy et al. [24] investigated the flow of upper convective Maxwell fluid past a rigid plate in continuous motion. Several authors [25–33] have solved many problems under generalized thermal theories. Zeeshan et al. [34], Elgazery et al. [35] and Bhatti et al. [36] have presented the solutions to some problems under various boundary conditions in porous mediums.

To the best of the Authors' knowledge, no information is available on the effects of an inclined magnetic field on heat and mass transfer in the turbulent squeeze flow of a viscoelastic fluid with an upper-convected Maxwell model. The present work aims to fill the gap in the existing literature. Therefore, in the present paper, we consider an inclined magnetic field and UCM squeezing flow of viscous fluid between parallel plates. We shall apply the shooting technique along with the Adams-Moulton method of fourth order to solve the similarity equations obtained from the governing boundary layer equations with the help of similarity transformation. The structure of the present paper is as follows. The problem is formulated in Section Two. The numerical solution for both fluid and temperature fields are presented in Section Three. Section Four contains results and discussions. The concluding remarks are eventually given in Section Five.

2. Materials and methods

An incompressible, 2-D unsteady UCM fluid flow, which is squeezed between two plates held parallel to each other (Fig. 1), along with the inclined magnetic field effect, has been considered.

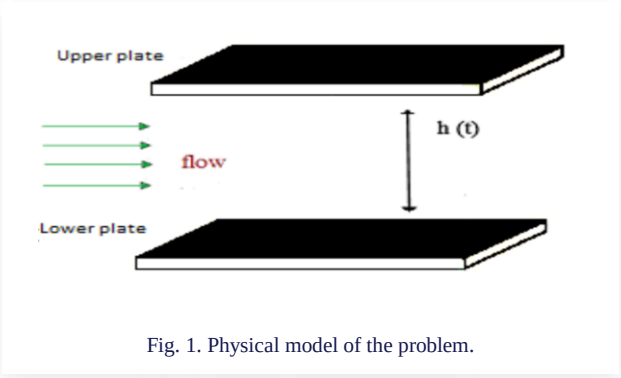

Fig. 1. Physical model of the problem.

The spacing between the plates is $y = l(1 - \alpha t)^{1/2} = h(t)$. For $\alpha > 0$, the two plates are squeezed until they touch $t = 1/\alpha$ and for $\alpha < 0$, the two plates are separated. Due to the viscous dissipation effect, the generation of heat due to friction caused by shear in the flow is retained. This effect is quite important in the case when the fluid is largely viscous or flowing at a high speed. This behaviour occurs at a high Eckert number. Mass transfer with a chemical reaction rate is accounted for. Moreover, the flow is considered symmetric. The continuity, momentum, energy and mass transfer in view of all these assumptions and approximations are given below [37]:

$$\frac{\partial u}{\partial x} + \frac{\partial v}{\partial y} = 0, \tag{1}$$

$$\left.\begin{aligned} \frac{\partial u}{\partial t} + u\frac{\partial u}{\partial x} + v\frac{\partial u}{\partial y} = -\frac{1}{\rho}\frac{\partial p}{\partial x} + \nu\left(\frac{\partial^2 u}{\partial x^2} + \frac{\partial^2 u}{\partial y^2}\right) + \\ + \frac{\sigma B_m^2}{\rho}\sin(\omega)\left(v\cos(\omega) - u\sin(\omega)\right) + \\ -\beta\left(u^2\frac{\partial^2 u}{\partial x^2} + v^2\frac{\partial^2 u}{\partial y^2} + 2uv\frac{\partial^2 u}{\partial x \partial y}\right) \end{aligned}\right\}, \tag{2}$$

$$\left.\begin{aligned} \frac{\partial v}{\partial t} + u\frac{\partial v}{\partial x} + v\frac{\partial v}{\partial y} = -\frac{1}{\rho}\frac{\partial p}{\partial y} + \nu\left(\frac{\partial^2 v}{\partial x^2} + \frac{\partial^2 v}{\partial y^2}\right) + \\ + \frac{\sigma B_m^2}{\rho}\sin(\omega)\left(v\cos(\omega) - u\sin(\omega)\right) + \\ -\beta\left(u^2\frac{\partial^2 v}{\partial x^2} + v^2\frac{\partial^2 v}{\partial y^2} + 2uv\frac{\partial^2 v}{\partial x \partial y}\right) \end{aligned}\right\}, \tag{3}$$

$$\left.\begin{aligned} \frac{\partial T}{\partial t} + u\frac{\partial T}{\partial x} + v\frac{\partial T}{\partial y} = \frac{k}{\rho C_p}\left(\frac{\partial^2 T}{\partial x^2} + \frac{\partial^2 T}{\partial y^2}\right) + \\ + \frac{\nu}{C_p}\left[4\left(\frac{\partial u}{\partial x}\right)^2 + \left(\frac{\partial u}{\partial y} + \frac{\partial v}{\partial x}\right)\right] \end{aligned}\right\}, \tag{4}$$

$$\frac{\partial C}{\partial t} + u\frac{\partial C}{\partial x} + v\frac{\partial C}{\partial y} = D\left(\frac{\partial^2 C}{\partial x^2} + \frac{\partial^2 C}{\partial y^2}\right) - K_1(t)C. \tag{5}$$

The boundary conditions for the above modelled problem are [37]:

$$\left.\begin{aligned} y=h(t):\ u=0, v=v_w=\frac{dh}{dt},\\ T=T_H,\ C=C_H,\\ y=0:\ u=\frac{\partial u}{\partial y}=\frac{\partial T}{\partial y}=\frac{\partial C}{\partial y}=0. \end{aligned}\right\} \quad (6)$$

Here, ρ is the fluid density, u and v are the velocities in the x and y directions, respectively, T denotes the temperature, C represents the concentration, p denotes the pressure, ν represents the kinematic viscosity, C_p is the specific heat, D denotes the coefficient of diffusion, and $B_m(t)=\frac{B_0}{(1-\alpha t)}, K_1(t)=\frac{k_1}{(1-\alpha t)}$ (see [25]) define the magnetic field and rate of reaction, which depend both on time.

A set of the following transformations is formed for the velocity components u and v, temperature T, concentration C and similarity variable η as [37]:

$$\left.\begin{aligned} u=\frac{\alpha x}{2(1-\alpha t)}f'(\eta), \quad v=\frac{-\alpha l}{\left[l(1-\alpha t)^{\frac{1}{2}}\right]}f(\eta),\\ \theta=\frac{T}{T_H}, \quad \phi=\frac{C}{C_H}, \quad \eta=\frac{y}{\left[l(1-\alpha t)^{\frac{1}{2}}\right]}, \end{aligned}\right\} \quad (7)$$

where the unknown function $f(\eta)$ represents the axial velocity component, $\theta(\eta)$ represents the temperature function and $\phi(\eta)$ is the concentration distribution. The new variables in Eq. (7) are submitted to the governing PDEs (1)–(5), and we get the following system of ODEs:

$$\left.\begin{aligned} f^{(iv)}(\eta)-\frac{S\left(\begin{matrix}3f^{"}(\eta)+\eta f'^{"}(\eta)+f'(\eta)f^{"}(\eta)\\ -f(\eta)f'^{"}(\eta)\end{matrix}\right)}{\left[1+S\lambda_r(f(\eta))^2\right]}+\\ -\frac{M^2\sin(\omega)\left(f^{"}(\eta)\sin(\omega)+2\delta\cos(\omega)\right)}{\left[1+S\lambda_r(f(\eta))^2\right]}+\\ -\frac{2S\lambda_r\left[f(\eta)\left(f^{"}(\eta)\right)^2+\left(f'(\eta)\right)^2f^{"}(\eta)\right]}{\left[1+S\lambda_r(f(\eta))^2\right]}=0 \end{aligned}\right\}, \quad (8)$$

$$\theta^{"}(\eta)+\mathrm{Pr}[S\left(f(\eta)\theta'(\eta)-\eta\theta'(\eta)\right)+ +\mathrm{Ec}\left(f'(\eta)\right)^2+\mathrm{Ec}(x)\left(f^{"}(\eta)\right)^2]=0, \quad (9)$$

$$\phi^{"}(\eta)+\mathrm{Sc}\left[\left(f(\eta)\phi'(\eta)-\eta\phi'(\eta)\right)-\gamma\phi(\eta)\right]=0. \quad (10)$$

The dimensionless boundary conditions are as follows:

$$\left.\begin{aligned} f(0)=0, \quad f^{"}(0)=1, \quad \theta'(0)=0, \quad \phi'(0)=0,\\ f(1)=1, \quad f'(1)=0, \quad \theta(1)=\phi(1)=1, \end{aligned}\right\} \quad (11)$$

where S is the squeeze number, Pr is the Prandtl number, Ec is the Eckert number, Sc is the Schmidt number, γ is the chemical reaction parameter, M is the magnetic parameter, λ_r is the viscoelastic parameter, Ec(x) is the local Eckert number, The various parameters utilized in the aforementioned equations can be expressed as follows:

$$\left.\begin{aligned} S=\frac{\alpha l^2}{2\nu}, \quad \mathrm{Pr}=\frac{\mu C_p}{k}, \quad \mathrm{Ec}=\frac{\alpha^2 l^2}{T_H C_p(1-\alpha t)}, \quad \mathrm{Sc}=\frac{\nu}{D},\\ \gamma=\frac{k_1 l^2}{\nu}, \quad M^2=\frac{\sigma B_0^2 l^2}{\rho\nu}, \quad \lambda_r=\frac{\alpha\beta}{2(1-\alpha t)},\\ \mathrm{Ec}(x)=\frac{\alpha^2 x^2}{4C_pT_H(1-\alpha t)^2}. \end{aligned}\right\} \quad (12)$$

It is important to note that the squeeze number S describes the movement of the plate ($S>0$ corresponds to the plates moving apart, while $S<0$ corresponds to the plates moving together) and Ec = 0 corresponds to the case when the viscous dissipation effect is absent, $\gamma>0$ represents the destructive chemical reaction and $\gamma<0$ represents the generative chemical reaction.

Expressions for the skin friction coefficient, local Nusselt number and local Sherwood number are as below [26]:

$$\left.\begin{aligned} C_f=\frac{\mu\left(\frac{\partial u}{\partial y}\right)\Big|_{y=h(t)}}{\rho v_w^2} \Rightarrow \frac{l^2}{x^2}(1-\alpha t)\mathrm{Re}_xC_f=f^{"}(1),\\ \mathrm{Nu}=\frac{-lk\left(\frac{\partial T}{\partial y}\right)\Big|_{y=h(t)}}{kT_H} \Rightarrow \sqrt{(1-\alpha t)}\mathrm{Nu}=-\theta'(1),\\ \mathrm{Sh}=\frac{-lD\left(\frac{\partial C}{\partial y}\right)\Big|_{y=h(t)}}{DC_H} \Rightarrow \sqrt{(1-\alpha t)}\mathrm{Sh}=-\phi'(1). \end{aligned}\right\} \quad (13)$$

3. Solution methodology

The system of ODEs (8)–(10) along with BCs (11) is solved numerically by utilizing the shooting technique with the Adams-Moulton method. A system of first order ODEs is required for the implementation of the shooting technique. The nonlinear differential equations are first decomposed into a system of first order differential equations. For this purpose, we introduce the new variables:

$$f=y_1, \quad f'=y_1'=y_2, \quad f^{"}=y_1^{"}=y_2'=y_3, \quad f^{"'}=y_4.$$

By using the above notations in Eq. (8), the following system of ODEs is obtained:

$$y_1'=y_2, \quad y_1(0)=0,$$

$$y_2'=y_3, \quad y_2(0)=r,$$

$$y_3'=y_4, \quad y_3(0)=0,$$

$$y_4'=\frac{\left[\begin{matrix}S(\eta y_4+3y_3+y_2y_3-y_1y_4)\\ +M^2\sin(\omega)(\sin(\omega)y_3+2\delta\cos(\omega)y_2)\\ +2S\lambda_r(y_2^2y_3+y_1y_3^2)\end{matrix}\right]}{1+S\lambda_ry_1^2}, \quad y_4(0)=s.$$

To solve the above initial value problem arising in the shooting technique, the Adams-Moulton method of the fourth order is used. Here the missing conditions r and S are to be determined so that:

$$\left.\begin{aligned} y_1(\eta_\infty,r,s)_{\eta=1}-1=0,\\ y_2(\eta_\infty,r,s)_{\eta=1}=0. \end{aligned}\right\} \quad (14)$$

To solve the above system of algebraic Eqs. (14), we use Newton's method which has the following iterative scheme:

$$\begin{pmatrix} r^{(k+1)} \\ s^{(k+1)} \end{pmatrix} = \begin{pmatrix} r^{(k)} \\ s^{(k)} \end{pmatrix} - \begin{pmatrix} \frac{\partial y_1}{\partial r} & \frac{\partial y_2}{\partial r} \\ \frac{\partial y_1}{\partial s} & \frac{\partial y_2}{\partial s} \end{pmatrix}^{-1}_{\eta=1} \begin{pmatrix} y_1(\eta, r^{(k)}, s^{(k)}) - 1 \\ y_2(\eta, r^{(k)}, s^{(k)}) \end{pmatrix}_{\eta=1}.$$

Here, k is the number of iterations ($k = 0, 1, 2, 3, \ldots$). The missing initial conditions r and S are updated by using Newton's scheme. The iterative procedure is stopped when the following criterion is met:

$$\max\{|r^{(k+1)} - r^{(k)}|, |s^{(k+1)} - s^{(k)}|\} < \in, \qquad (15)$$

where $\in$ denotes a small positive number.

The step size is taken as $\Delta\eta = 0.01$. The process is repeated until we obtain the result correct up to the desired accuracy of 10^{-7}, which fulfils the convergence criterion.

Now Eq. (15) will be treated similarly by considering f as a known function. For this, let us denote θ by y_{13} and $\theta' = y'_{13}$ by y_{14}.

By using the above notations in Eq. (15), we get the system of equations:

$$y'_{13} = y_{14}, \qquad y_{13}(0) = m,$$

$$y'_{14} = \mathrm{Pr}S(\eta y_{14} - y_1 y_{14}) - \mathrm{Pr}\mathrm{E}c y_2^2 - \mathrm{Pr}\mathrm{E}c(x), \quad y(0) = 0.$$

The above initial value problem will be numerically solved by the fourth order Adams-Moulton method. In the above initial value problem, the missing condition m is to be chosen such that:

$$y_{13}(\eta, m)_{\eta=1} - 1 = 0. \qquad (16)$$

To solve the above algebraic Eq. (16), we use Newton's method which has the following iterative scheme:

$$m^{(k+1)} = m^{(k)} - \left(\frac{\partial y_{13}}{\partial m}\right)^{-1} \left(y_{13}(\eta, m^{(k)})_{\eta=1} - 1\right).$$

To incorporate Newton's method, we further use the following notations:

$$\frac{\partial y_{13}}{\partial m} = y_{15}, \qquad \frac{\partial y_{14}}{\partial m} = y_{16}.$$

As a result of these new notations, the Newton's iterative scheme gets form:

$$m^{(k+1)} = m^{(k)} - \left(y_{15}(\eta, m^{(k)})_{\eta=1}\right)^{-1} \left(y_{13}(\eta, m^{(k)})_{\eta=1} - 1\right). \qquad (17)$$

Here, k is the number of iterations ($k = 0, 1, 2, 3, \ldots$). Now differentiating the above system of two first order ODEs with respect to m, we get another system of four ODEs. Writing all these four ODEs together, we have the following initial value problem (IVP):

$$y'_{13} = y_{14}, \qquad y_{13}(0) = m,$$

$$y'_{14} = \mathrm{Pr}\,S\,(\eta y_{14} - y_1 y_{14}) - \mathrm{Pr}\mathrm{E}c y_2^2 - \mathrm{Pr}\mathrm{E}c(x) y_3^2,$$

$$y_{14}(0) = 0,$$

$$y'_{15} = y_{16}, \qquad y_{15}(0) = 1,$$

$$y'_{16} = \mathrm{Pr}\,S\,(\eta y_{16} - y_1 y_{14}), \qquad y_{16}(0) = 0.$$

The Adams-Moulton method of the fourth order has been used to solve the IVP consisting of the above four ODEs for some suitable choices of m. The missing condition m is updated by using Newton's scheme (17). The iterative procedure is stopped when the following condition is met:

$$|m^{(k+1)} - m^{(k)}| < \in,$$

for an arbitrarily small positive value of $\in$. Throughout this article $\in$ has been taken as 10^{-8}.

In a similar manner, Eq. (10) can be treated numerically by the shooting techniques by considering f as a known function.

4. Results and discussion

This section examines how different physical factors affect the ranges of velocity, temperature, and concentration. It has been given and examined how the dimensionless mathematical model can be solved numerically. Mustafa et al. [37] used the HAM method for the numerical solution of the discussed model. In the present survey, the shooting method along with the Adams-Moulton method has been opted for reproducing the solution. The present results will be compared with those of [37] for verification of the code. The impact of different parameters, e.g. squeezing parameter S, Pr, Sc, γ and Ec is observed graphically.

Figures 2 and 3 show the impact of S on the dimensionless velocity profile. It can be noted that the fluid velocity reduces with the increasing values of the squeezing parameter.

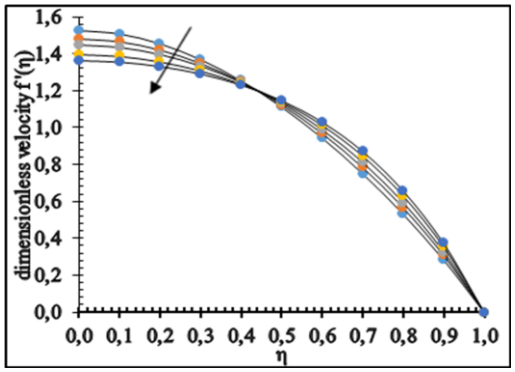

Fig. 2. Influence of $S = -1.0, -0.5, 0.01, 1.0, 2.0$ on $f'(\eta)$ for $\mathrm{Pr} = M = \mathrm{Ec} = \mathrm{Ec}(x) = \mathrm{Sc} = \gamma = 1$, $\delta = \lambda_r = 0.2$, $\omega = \pi/4$.

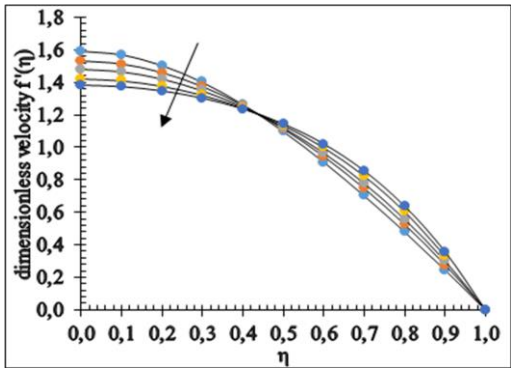

Fig. 3. Influence of $S = -1.0, -0.5, 0.01, 1.0, 2.0$ on $f'(\eta)$ for $\mathrm{Pr} = M = \mathrm{Ec} = \mathrm{Ec}(x) = \mathrm{Sc} = \gamma = 1$, $\delta = \lambda_r = 0.2$, $\omega = \pi/6$.

Figures 4 and 5 present the impact of both the positive and negative squeezing parameters on the temperature distribution. Greater values of S give a noteworthy decrease in the temperature profile. Physically, an increase in S can be associated with a decrease in the kinematic viscosity, an increase in the distance between the plates and an increase in the speed at which the plate moves.

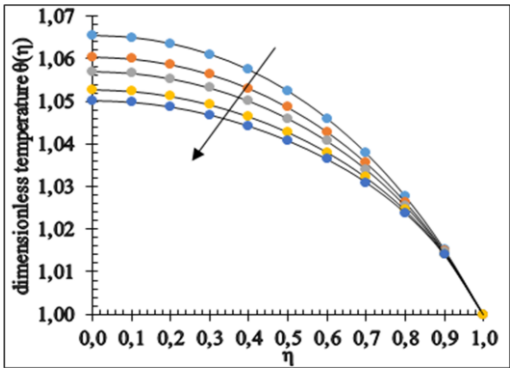

Fig. 4. Influence of $S = -1.0, -0.5, 0.01, 1.0, 2.0$ on $\theta(\eta)$ for Pr = M = Ec = Ec(x) = 0.2, Sc = γ = 1, $\delta = \lambda_r$ = 0.2, $\omega = \pi/4$.

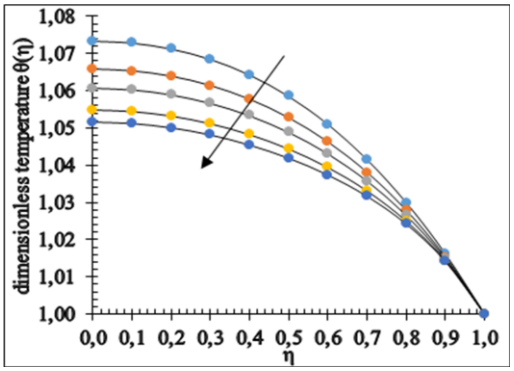

Fig. 5. Influence of $S = -1.0, -0.5, 0.01, 1.0, 2.0$ on $\theta(\eta)$ for Pr = M = Ec = Ec(x) = 0.2, Sc = γ = 1, $\delta = \lambda_r$ = 0.2, $\omega = \pi/6$.

Figures 6 and 7 show the impact of Pr on the field $\theta(\eta)$. The field $\theta(\eta)$ is rising due to the viscous dissipation effect. The Prandtl number Pr < 1 describes the liquid materials with a high thermal diffusivity but low viscosity, whereas the viscosity of liquid materials is high for the Prandtl number Pr > 1.

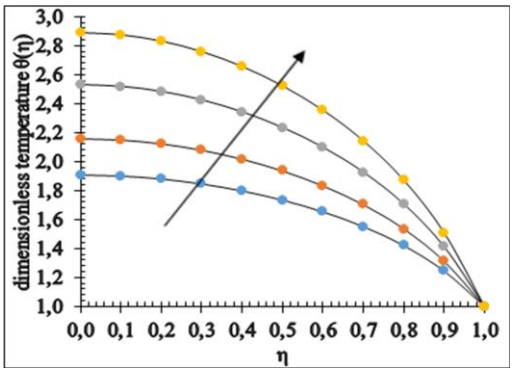

Fig. 6. Influence of Pr = 0,7, 0.9, 1.2, 1,5 on $\theta(\eta)$ for S = M = Ec = Ec(x) = Sc = γ = 1, $\delta = \lambda_r$ = 0.2, $\omega = \pi/4$.

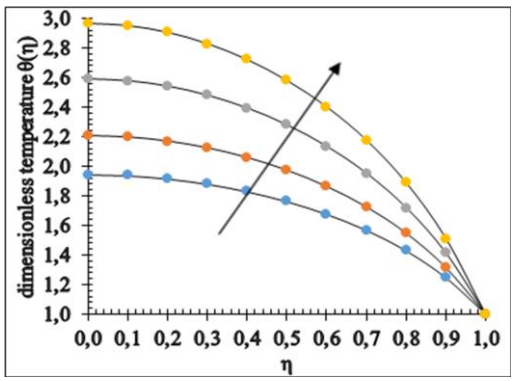

Fig. 7. Influence of Pr = 0,7, 0.9, 1.2, 1,5 on $\theta(\eta)$ for S = M = Ec = Ec(x) = Sc = γ = 1, $\delta = \lambda_r$ = 0.2, M = 3, $\omega = \pi/6$.

Figures 8 and 9 are delineated to show the impact of Ec on the temperature field $\theta(\eta)$. These figures describe that on the rising estimations of Ec, the temperature profile is also increased. Thus, the compactness of the thermal layer at the boundary is reduced by the increasing estimations of Pr and Ec.

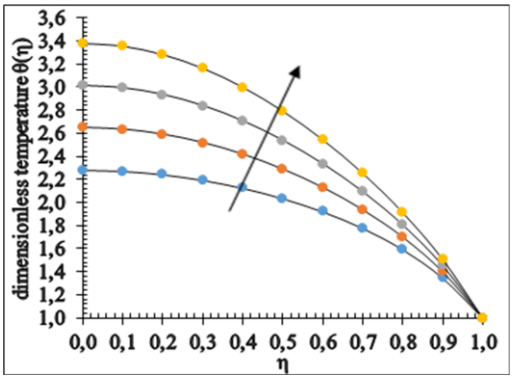

Fig. 8. Influence of Ec = 1.0, 1.5, 2.0, 2,5 on $\theta(\eta)$ for S = Pr = Ec(x) = Sc = γ = 1, $\delta = \lambda_r$ = 0.2, M = 3, $\omega = \pi/4$.

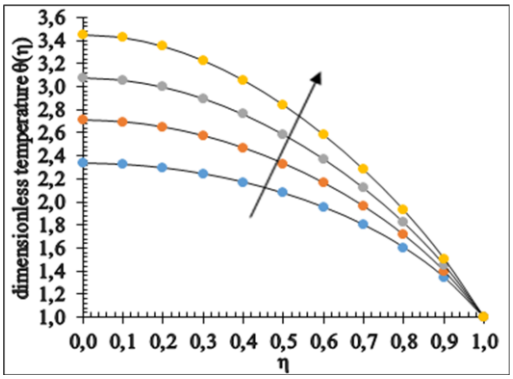

Fig. 9. Influence of Ec = 1.0, 1.5, 2.0, 2,5 on $\theta(\eta)$ for S = Pr = Ec(x) = Sc = γ = 1, $\delta = \lambda_r$ = 0.2, M = 3, $\omega = \pi/6$.

Figure 10 presents the temperature distribution for different values of the magnetic parameter M.

Figure 11 shows the behaviour of the temperature profile for the increasing values of the inclination angle ω of the applied

magnetic field. So, the influence of the magnetic inclination angle on the temperature profile of a fluid is similar to that of the magnetic parameter. Thus, in practical applications related to controlling the momentum and heat transfer of fluid in squeezing flow, the effects produced by changing the magnetic field strength can also be approximately achieved through adjusting the inclination angle of the magnetic field.

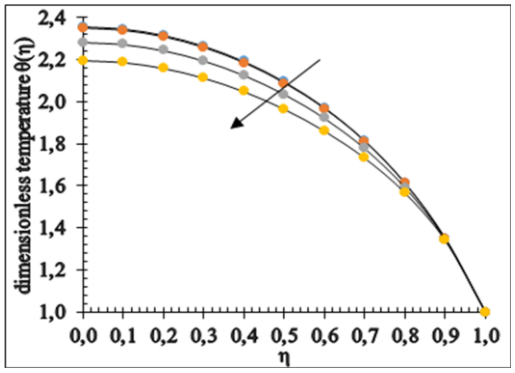

Fig. 10. Influence of M = 0, 1.0, 3.0, 5.0 on $\theta(\eta)$ for S = Pr = Ec = Ec(x) = Sc = γ = 1, $\delta = \lambda_r$ = 0.2, M = 3, $\omega = \pi/4$.

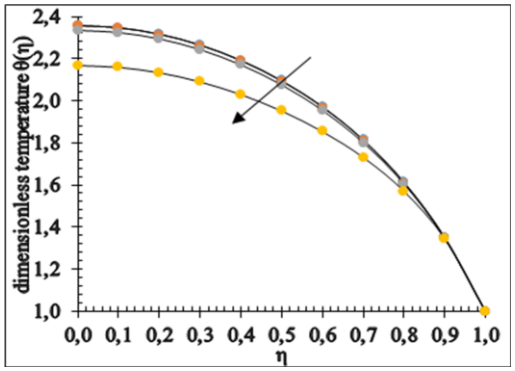

Fig. 11. Influence of ω = 0, $\pi/8$, $\pi/6$, $\pi/4$, $\pi/2$ on $\theta(\eta)$ for S = Pr = Ec = Ec(x) = Sc = γ = 1, $\delta = \lambda_r$ = 0.2, M = 3.

Figures 12 and 13 are to show the impact of S on the concentration field ϕ. A similar trend is noticed for the concentration profile as for the case of temperature field.

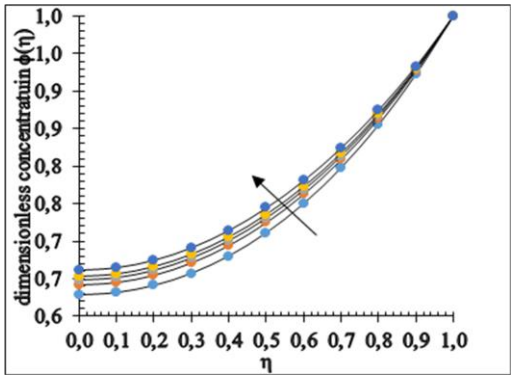

Fig. 12. Influence of S = −1.5, −0.5, 0.01, 0.5, 1.5 on $\phi(\eta)$ for Pr = M = Ec = Ec(x) = 0.2, Sc = γ = 1, $\delta = \lambda_r$ = 0.2, $\omega = \pi/4$.

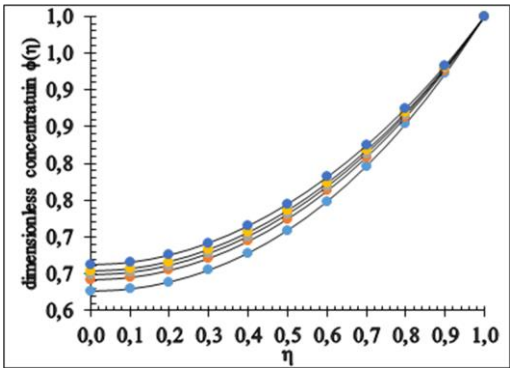

Fig. 13. Influence of S = −1.5, −0.5, 0.01, 0.5, 1.5 on $\phi(\eta)$ for Pr = M = Ec = Ec(x) = 0.2, Sc = γ = 1, $\delta = \lambda_r$ = 0.2, $\omega = \pi/6$.

The outcomes of Sc on the field ϕ are presented in Figs. 14 and 15. It can be noted that the molecular diffusivity turns more fragile, and the boundary layer thickness ends up slenderer because of the gradual increase in Sc.

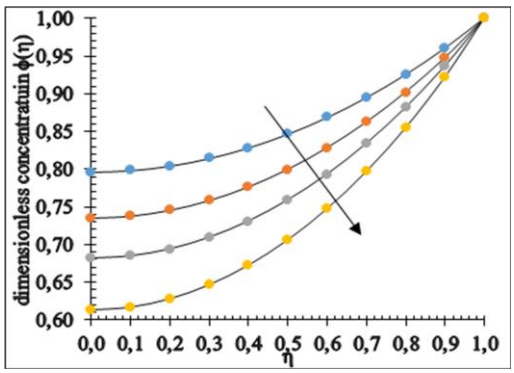

Fig. 14. Influence of Sc = 0.5, 0.7, 0.9, 1.2 on $\phi(\eta)$ for Pr = Ec = Ec(x) = γ = 1, $\delta = \lambda_r$ = 0.2, M = 3, $\omega = \pi/4$.

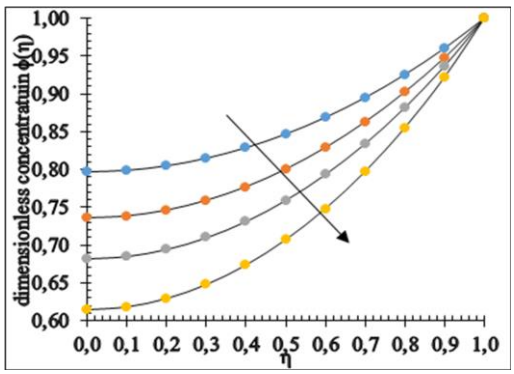

Fig. 15. Influence of Sc = 0.5, 0.7, 0.9, 1.2 on $\phi(\eta)$ for Pr = Ec = Ec(x) = γ = 1, $\delta = \lambda_r$ = 0.2, M = 3, $\omega = \pi/6$.

Figures 16 and 17 delineate the impact of concentration fields. For $\gamma > 0$, the concentration field ϕ declines significantly, whereas an increase in the concentration profile ϕ is very much visible for $\gamma < 0$. Steeper curves are observed when larger estimations of the reaction are accompanied by severe conditions, as shown in Figs. 16 and 17.

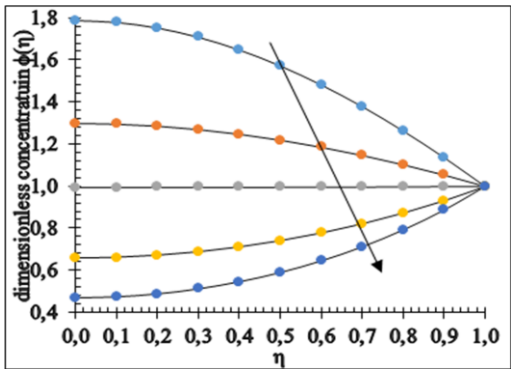

Fig. 16. Influence of $\gamma = -1.0, -0.5, 0.01, 1.0, 2.0$ on $\phi(\eta)$ for Pr = Ec = Ec(x) = S = Sc = 1, $\delta = \lambda_r = 0.2$, $M = 3$, $\omega = \pi/4$.

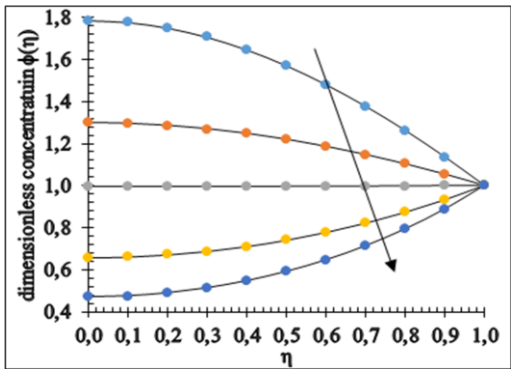

Fig. 17. Influence of $\gamma = -1.0, -0.5, 0.01, 1.0, 2.0$ on $\phi(\eta)$ for Pr = Ec = Ec(x) = S = Sc = 1, $\delta = \lambda_r = 0.2$, $M = 3$, $\omega = \pi/6$.

The numerical results of the coefficient of skin friction, the Sherwood number and Nusselt number for the distinct values of squeezing parameter S with some fixed parameters are shown in Tables 1−3.

Table 1. Skin friction coefficient for different parameters.

S	M	ω	δ	λ_r	$-f''(1)$	
					Mustafa et al. [37]	Present
-1.0	3.0	$\pi/4$	0.2	0.2	3.036639	3.037298
-0.5					3.357444	3.357991
0.01					3.612109	3.612580
0.5					3.808987	3.809395
2.0					4.232647	4.232942

Table 2. Sherwood number for $\omega = \pi/4$ rad, $M = 3.0$, $\lambda_r = \delta = 0.2$.

S	Sc	γ	$-\phi'(1)$	
			Mustafa et al. [37]	Present
-1.0	1.0	1.0	0.800351	0.8002988
-0.5			0.779759	0.7451639
0.01			0.761250	0.7612504
0.5			0.745138	0.7451639
2.0			0.702388	0.7024820

Table 3. Nusselt number for $\omega = \pi/4$ rad, $M = 3.0$, $\lambda_r = \delta = 0.2$.

S	Pr	Ec	Ec(x)	$-\theta'(1)$	
				Mustafa et al. [37]	Present
-1.0	0.2	0.2	0.2	0.170218	0.1701446
-0.5				0.168694	0.1686023
0.01				0.168541	0.1684339
0.5				0.169009	0.1688881
2.0				0.171515	0.1713616
2.0	0.4	0.2	0.2	0.339028	0.3387297
	0.6			0.502699	0.5022627
	0.8			0.662681	0.6621146
2.0	0.2	0.4	0.2	0.215831	0.2156981
		0.6		0.260147	0.2600345
		0.8		0.304463	0.3043713
0.2	0.2	0.2	0.4	0.298714	0.2983872
			0.6	0.425913	0.4254117
			0.8	0.553112	0.5524375

5. Conclusions

This article presents the simulation effects of heat and mass transfer on the UCM flow of a viscous fluid between parallel plates studied by considering the inclined magnetic field effect in the velocity equation. The set of nonlinear momentum, energy and concentration equations are transformed into the dimensionless ODEs by an appropriate transformation. Numerical solutions are obtained by using the shooting technique with the Adams-Moulton method. Our results are in excellent agreement with the existing numerical literature results. The influence of distinct physical parameters such as the Eckert number (Ec), Schmidt number (Sc), squeezing parameter (S), Prandtl number (Pr) and the chemical reaction parameter (γ) on the velocity profile, temperature field and the concentration profile are elaborated in the graphical and tabular form. The above-mentioned analysis of the UCM flow has led us to the following conclusions:

- A decrease in the temperature profile is noted with the increasing values of the squeezing parameter;
- It is observed that an increment in the temperature occurs with the increasing values of the Eckert number;
- An increment in the Schmidt number is observed to decrease the concentration profile;
- The temperature distribution decreases due to the boosting value of the magnetic parameter;
- When the values of the chemical reaction parameter are increased, the concentration profile decreases, whereas when the chemical reaction parameter is decreased, the concentration profile increases;
- The problem can be extended by a stretching surface in different types of fluids for instance a Maxwell nanofluid;
- The problem can be further extended for the cylindrical and rotating disk geometries. Some other parameters can also be included like porous media, yielding Soret and Dufour effects;

– Different numerical techniques can be utilized to solve fluid flow problems.

Acknowledgements

The authors acknowledge the constructive suggestions received from the reviewers and the editor which led to definite improvements in the paper.

References

[1] Duwairi, H., Tashtoush, B., & Damseh, R.A. (2004). On heat transfer effects of a viscous fluid squeezed and extruded between two parallel plates. *Heat and Mass Transfer*, 41(2), 112−117. doi: 10.1007/s00231-004-0525-5

[2] Hsiao, K.-L. (2017). Combined electrical MHD heat transfer thermal extrusion system using Maxwell fluid with radiative and viscous dissipation effects. *Applied Thermal Engineering*, 112, 1281−1288. doi: 10.1016/j.applthermaleng.2016.08.208

[3] Ahmadi, A.R., Zahmatkesh, A., Hatami, M., & Ganji, D.D. (2014). A comprehensive analysis of the flow and heat transfer for a nanofluid over an unsteady stretching at plate. *Powder Technology*, 258, 125−133. doi: 10.1016/j.powtec.2014.03.021

[4] Afify, A.A. (2004). MHD free convective flow and mass transfer over a stretching sheet with chemical reaction. *Heat and Mass Transfer*, 40(6−7), 495−500. doi: 10.1007/s00231-003-0486-0

[5] Bhatta, D.P., Mishra, S.R., & Dash, J.K. (2019). Unsteady squeezing flow of water-based nanofluid between two parallel disks with slip effects: Analytical approach. *Heat Transfer Asian Research*, 48(5), 1575−1594. doi: 10.1002/htj.21447

[6] Adesanya, S.O., Ogunseye, H.A., & Jangili, S. (2018). Unsteady squeezing flow of a radiative Eyring Powell fluid channel flow with chemical reactions. *International Journal of Thermal Sciences*, 125, 440−447. doi: 10.1016/j.ijthermalsci.2017.12.013

[7] Farooq, M., Ahmad, S., Javed, M., & Anjum, A. (2019). Melting heat transfer in squeezed nanofluid flow through Darcy Forchheimer medium. *Journal of Heat Transfer*, 141, 012402. doi: 10.1115/1.4041497

[8] Hayat, T., Nawaz, M., Hendi, A.A. & Asghar, S. (2011). MHD squeezing flow of a micropolar fluid between parallel disks. *Journal of Fluids Engineering*, 133(11), 111206. doi: 10.1115/1.4005197

[9] Mahmood, M., Asghar, S., & Hossain, M.A. (2007). Squeezed flow and heat transfer over a porous surface for viscous fluid. *Heat and Mass Transfer*, 44(2), 165−173. doi: 10.1007/s00231-006-0218-3

[10] Mohyud-Din, S.T., Khan, S.I., Khan, U., Ahmed, N., & Xiao-Jun, Y. (2018). Squeezing flow of MHD fluid between parallel disks. *International Journal for Computational Methods in Engineering Science and Mechanics*, 19(1), 42−47. doi: 10.1080/15502287

[11] Ojjela, O., Ramesh, K., & Das, S.K. (2018). Second law analysis of MHD squeezing flow of Casson fluid between two parallel disks. *International Journal of Chemical Reactor Engineering*, 16(6). doi: 10.1515/ijcre-2017-0163

[12] Sheikholeslami, M., Ganji, D., & Ashorynejad, H.(2013). Investigation of squeezing unsteady nanofluid flow using ADM. *Powder Technology*, 239, 259−265. doi: 10.1016/j.powtec.2013.02.006

[13] Gholinia, M., Hosseinzadeh, K., Mehrzadi, H. Ganji, D., & Ranjbar, A. (2019). Investigation of MHD Eyring Powell fluid flow over a rotating disk under effect of homogeneous-heterogeneous reactions. *Case Studies in Thermal Engineering*, 13, 100356. doi: 10.1016/j.csite.2018.11.007

[14] Hayat, T., Yousaf, A., Mustafa, M., & Obaidat, S. (2012). MHD squeezing flow of second-grade fluid between two parallel disks. *International Journal for Numerical Methods in Fluids*, 69(2), 399−410. doi: 10.1002/fld.2565

[15] Jha, B.K. & Aina, B. (2018). Magnetohydrodynamic natural convection flow in a vertical micro-porous channel in the presence of induced magnetic field. *Communications in Nonlinear Science and Numerical Simulation*, 64, 14−34. doi: 10.1016/j.cnsns.2018.04.004

[16] Khan, U., Ahmed, N., & Mohyud-Din, S.T. (2018). Analysis of magnetohydrodynamic flow and heat transfer of Cu-water nanofluid between parallel plates for different shapes of nanoparticles. *Neural Computing and Applications*, 29(1), 695−703 doi: 10.1007/s00521-016-2596-x

[17] Mabood, F., Shateyi, S., Rashidi, M., Momoniat, E., &. Freidoonimehr, N. (2016). MHD stagnation point flow heat and mass transfer of nanofluids in porous medium with radiation, viscous dissipation and chemical reaction. *Advanced Powder Technology*, 27(2), 742−749. doi: 10.1016/j.apt.2016.02.033

[18] Siddiqui, A.M., Irum, S., & Ansari, A.R. (2008). Unsteady squeezing flow of a viscous MHD fluid between parallel plates, a solution using the homotopy perturbation method. *Mathematical Modelling and Analysis*, 13(4), 565–576. doi: 10.3846/1392-6292.2008.13.565-576

[19] Abbasi, M., Khaki, M., Rahbari, A., Ganji, D., & Rahimipetroudi, I. (2016). Analysis of MHD flow characteristics of a UCM viscoelastic flow in a permeable channel under slip conditions. *Journal of the Brazilian Society of Mechanical Sciences and Engineering*, 38(3), 977−988. doi: 10.1007/s40430-015-0325-5

[20] Choi, J., Rusak, Z., & Tichy, J. (1999). Maxwell fluid suction flow in a channel. *Journal of Non-Newtonian Fluid Mechanics*, 85(2−3), 165−187. doi: 10.1016/S0377-0257(98)00197-9

[21] Hayat, T., & Abbas, A. (2008). Channel flow of a Maxwell fluid with chemical reaction. *Zeitschrift four angewandte Mathematik und Physik*, 59(1), 124−144. doi: 10.1007/s00033-007-6067-1

[22] Mukhopadhyay, S., & Vajravelu, K. (2012). Effects of transpiration and internal heat generation/absorption on the unsteady flow of a Maxwell fluid at a stretching surface. *Journal of Applied Mechanics*, 79(4), 044508. doi: 10.1115/1.4006260

[23] Prasad, A., Sujatha, A., Vajravelu, K., & Pop, I. (2012). MHD flow and heat transfer of a UCM fluid over a stretching surface with variable thermophysical properties. *Meccanica*, 47(6), 1425−1439. doi: 10.1007/s11012-011-9526-x

[24] Sadeghy, K., Najafi, A.H., & Saffaripour, M. (2005). Sakiadis flow of an upper-convected Maxwell fluid. *International Journal of Non-Linear Mechanics*, 40(9), 1220−1228. doi: 10.1016/j.ijnonlinmec.2005.05.006

[25] Hayat, T., Qasim, M., & Abbas, Z. (2010). Radiation and mass transfer effects on magnetohydrodynamic unsteady flow induced by a shrinking sheet. *Z Naturforsch*, 65(3), 231–239. doi: 10.1515/zna-2010-0312

[26] Abbas, I.A. (2007). Finite element analysis of the thermoelastic interactions in an unbounded body with a cavity. *Forschung Im Ingenieurwesen*, 71, 215–222. doi: 10.1007/s10010-007-0060-x

[27] Alzahrani, F., Hobiny, A., Abbas, I., & Marin, M. (2020). An Eigenvalues Approach for a Two-Dimensional Porous Medium Based Upon Weak, Normal and Strong Thermal Conductivities. *Symmetry*, 12(5), 848. doi: 10.3390/sym12050848

[28] Abbas I.A., & Kumar, R. (2016). 2D deformation in initially stressed thermoelastic half-space with voids. *Steel and Composite Structures*, 20(5), 1103−1117. doi: 10.12989/scs.2016.20.5.1103

[29] Zenkour, A., & Abbas, I.A. (2014). Nonlinear Transient Thermal Stress Analysis of Temperature-Dependent Hollow Cylinders

Using a Finite Element Model. *International Journal of Structural Stability and Dynamics*, 14(6), 1450025. doi: 10.1142/S0219455414500254

[30] Abbas, I., Hobiny, A., & Marin M. (2020). Photo-thermal interactions in a semi-conductor material with cylindrical cavities and variable thermal conductivity. *Journal of Taibah University for Science*, 14(1), 1369−1376. doi: 10.1080/16583655.2020.1824465

[31] Marin, M., Hobiny, A., & Abbas, I. (2021). The Effects of Fractional Time Derivatives in Por thermoelastic Materials Using Finite Element Method. *Mathematics*, 9(14), 1606. doi: 10.3390/math9141606

[32] Narender, G., Govardhan, K., & Sreedhar Sarma, G. (2020). Magnetohydrodynamic stagnation point on a Casson nanofluid flow over a radially stretching sheet. *Beilstein Journal of Nanotechnology*, 11, 1303–1315. doi: 10.3762/bjnano.11.114

[33] Narender, G., Govardhan, K., & Sreedhar Sarma, G. (2021). MHD Casson Nanofluid Past a Stretching Sheet with the Effects of Viscous Dissipation. Chemical Reaction and Heat Source/Sink. *Journal of Applied Computational Mechanics*, 7(4): 2040–2048. doi: 10.22055/JACM.2019.14804

[34] Zeeshan, A., Ahmad, M., Ellahi, R., Sait, S.M., & Shehzad, N. (2023). Hydromagnetic flow of two immiscible nanofluids under the combined effects of Ohmic and viscous dissipation between two parallel moving plates. *Journal of Magnetism and Magnetic Materials*, 575(1), 170741. doi: 10.1016/j.jmmm.2023.170741

[35] Elgazery, N.S., Elelamy, A.F., Bobescu, E., & Ellahi, R. (2021). How do artificial bacteria behave in magnetized nanofluid with variable thermal conductivity: application of tumor reduction and cancer cells destruction. *International Journal of Numerical Methods for Heat and Fluid Flow*, 32(9), 2982−3006. doi: 10.1108/HFF-11-2021-0722

[36] Bhatti, M.M., Marin, M., Ellahi, R., & Fudulu, I.M. (2023). Insight into the dynamics of EMHD hybrid nanofluid (ZnO/CuO-SA) flow through a pipe for geothermal energy applications. *Journal of Thermal Analysis and Calorimetry*, 24, 14261–14273. doi: 10.1007/s10973-023-12565-8

[37] Mustafa, M., Hayat, T., & Obaidat, S. (2012). On heat and mass transfer in the unsteady squeezing flow between parallel plates. *Meccanica*, 47(7), 1581−1589. doi: 10.1007/s11012-012-9536-3